infrastructures

MDPI

Article

Statistical Analysis of the Effective Friction Angle of Sand Tailings from Germano Dam

Leonardo De Bona Becker *, Maria do Carmo Reis Cavalcanti and Alfredo Affonso Monteiro Marques

Department of Civil Construction-Geotechnics, Federal University of Rio de Janeiro, Rio de Janeiro 21941-901, Brazil

* Correspondence: leonardobecker@poli.ufrj.br; Tel.: +55-21-39387437

Abstract: Tailings dam accidents emphasize the importance of an adequate understanding of the strength parameters of tailings to improve the efficiency and effectiveness of the design, construction, and operation of such structures. Usually, the tailings strength is addressed in a deterministic manner. However, a statistical approach would better represent their behavior due to its inherent heterogeneity. The literature about tailings strength distribution is relatively rare or superficial, which impairs the probabilistic analyses which are essential for risk management. Therefore, this article focuses on the probability density function (PDF) of the effective friction angle (ϕ') of iron ore tailings from the reservoir of Germano dam, Mariana, Brazil, based on data from publicly available CPTu tests. The influence of the relative density (D_r), and the presence of plastic layers amidst the sand tailings on the strength of the sand are also discussed herein. Several correlations were employed to estimate ϕ' and D_r. According to the results, the presence of plastic layers influences the estimated properties, and the relative density has a log-normal distribution. The effective friction angle, on the other hand, presents a normal distribution.

Keywords: tailings dams; tailings; effective friction angle; relative density; probabilistic approach; CPTu

Citation: Becker, L.D.B.; Cavalcanti, M.d.C.R.; Marques, A.A.M. Statistical Analysis of the Effective Friction Angle of Sand Tailings from Germano Dam. *Infrastructures* **2023**, *8*, 61. https://doi.org/10.3390/infrastructures8030061

Academic Editor: Paolo Simonini

Received: 22 December 2022
Revised: 7 March 2023
Accepted: 13 March 2023
Published: 22 March 2023

1. Introduction

The acceleration of urban growth close to mining sites is a significant challenge. The collapse of tailings dams in the cities of Mariana [1] and Brumadinho caused hundreds of deaths and billions of dollars in damages. As the height and volume of tailings dams increase, and their distance to the nearest cities shortens, the potential consequences of failures become more critical. In that context, governments and society increasingly demand risk assessment and management.

Probabilistic analysis of slope stability became more widespread with the increasing availability of high-capacity computers that have led to many advances in recent decades e.g., [2–10].

Recent guidelines have included provisions for risk assessment [11,12], and it is believed that probabilistic analysis of the slope stability of tailings dams will become mainstream soon. Despite that, stability analysis based on deterministic safety factors is still the most common and usually the only mandatory study.

There are several definitions of risk and equations to assess it. According to Varnes [13], the "Total Risk" (R) of an adverse event, such as deaths and damages due to the collapse of a tailings dam caused by a slope failure mechanism, may be defined as the product of the probability of occurrence of the slope failure (also called "susceptibility", S), by the "consequences" (C) of the event, and the degree of loss of a given element or set of elements at risk resulting from the occurrence of the adverse event ("vulnerability", V), i.e., $R = V \cdot S \cdot C$).

To quantitatively assess the failure probability, it is necessary to conduct a probabilistic stability analysis, which depends on many factors. Given the significant variability of the properties of the materials stored in tailings dams and the random nature of

their deposition, the main influence in the susceptibility is usually the distribution of tailings strength.

Unfortunately, studies of tailings strength distribution are rare, hindering the use of probabilistic analysis.

Accidents involving the failure of iron ore tailings dams in Brazil, particularly the most recent ones in Mariana (2015) and Brumadinho (2019), raised discussions on the paramount importance of an adequate understanding of the behavior of tailings. These failures caused hundreds of deaths and massive environmental damages since tailings flooded large areas, traveled hundreds of kilometers, and reached the ocean [1,14–17].

The present work aims to study the intrinsic variability of the iron ore sand tailings by assessing the friction angle's probability distribution and the sand tailings' relative density based on data from CPTu tests carried out in the reservoir.

Since the tailings disposal procedure leads to heterogeneous stratigraphy with embedded randomly distributed layers of plastic, clay-like, fine tailings, whose presence affects the CPTu results, the study was carried out for four different scenarios. In some scenarios, the outliers or the results affected by the plastic layers were removed from the data to assess their impact on the ϕ' PDF. This innovative approach allowed to better understand the shear strength of sand tailings and minimize the influence of the clay-like layers.

2. Materials and Methods

The sand tailings from the Germano dam reservoir discussed herein are classified as silty sand. Usually, the clay content is zero, and the silt content ranges from 30% to 50% [1,18,19]. It should be noted that the Fundão dam and Germano dam received tailings from the same mine. Figure 1 presents an image obtained by an electronic microscope and Figure 2 shows an image of the same tailings by the optical microscope.

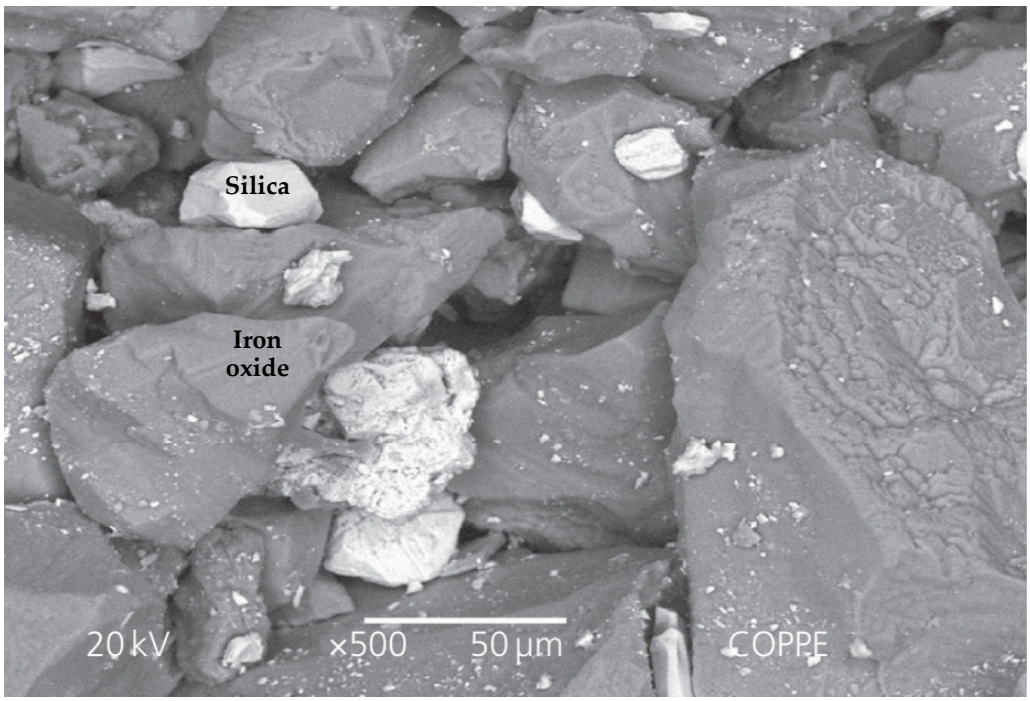

Figure 1. MEV photographs of the Fundão dam tailings—500× enlargement [20].

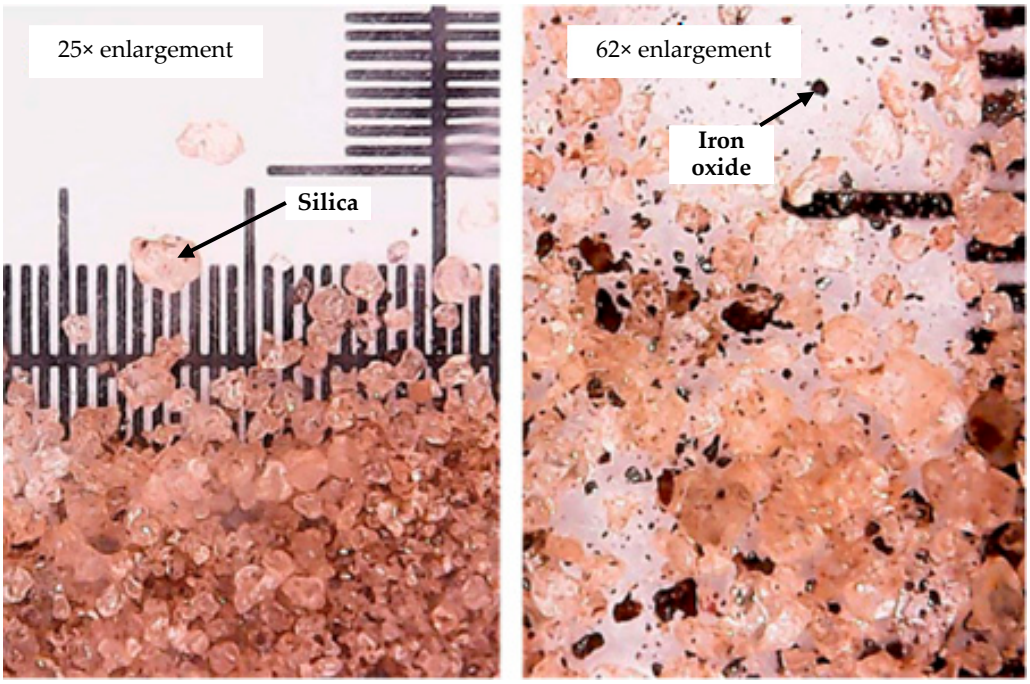

Figure 2. Optical microscope photographs of the Fundão dam tailings [19].

2.1. Laboratory Studies on the Shear Strength of Iron Ore Tailings from Minas Gerais State, Brazil

Table 1 presents the effective friction angle of iron ore tailings from several dams in Minas Gerais state.

Table 1. Effective friction angle of iron ore tailings from Minas Gerais state, Brazil.

Dam (City/State)	ϕ' (°)	Reference
Córrego do Doutor (Ouro Preto/MG)	30–34	[18]
Campo Grande (Mariana/MG)	32–45	[18]
Gongo Soco (Barão de Cocais/MG)	26–32	[18]
Pontal (Itabira/MG)	32–36	[18]
Fundão dam (Mariana/MG)	28–36	[1,19–24]

Flórez et al. [20] present the characteristics of disturbed tailings samples obtained in the Fundão dam two years before its collapse. The characterization included chemical fluorescence (XRF), mineralogical X-ray diffractometry (XRD), scanning electron microscope (SEM), and particle size analysis. The tailings are silty sand composed of quartz, iron oxides, hematite, and goethite. The fines are composed entirely of the silt fraction. This sample has been used in several studies. For example, Becker and Barbosa [21] present eleven triaxial compression tests (drained and undrained) in remolded samples that reached the critical state. The friction angle at the critical state (ϕ'_{cs}) equals 33°, regardless of the drainage condition of the test. Becker et al. [19] described a photography technique to determine axial and radial strains in triaxial extension tests. They used another batch of the same tailings sample obtained by [20]. The critical state friction angle in drained extension was approximately equal to the critical state friction angle in drained compression (i.e., $\phi'_{cs,tc}$ = 34.3° and $\phi'_{cs,te}$ = 34.8°). Twelve direct shear tests on remolded tailings samples obtained from the Fundão dam two years before the dam's collapse were performed by Quintelas et al. [22]. The samples were classified as silty sand. Four relative densities (D_r = 98%, 81%, 58%, and 35%) were used in the tests. The peak and constant volume friction angles were 37° and 33°, respectively, for effective vertical stresses between 100 kPa and 400 kPa. Quirino et al. [23] performed ring shear tests to study the influence of the fines content (FC) on the friction angle of this sample of sand tailings. Five proportions

of sand and silt were used (FC ranged from 0 to 100% and was entirely composed of the parcel passing the #200 sieve). The minimum and maximum friction angles were 29° and 31°, respectively.

Thirteen triaxial compression tests on remolded sand tailings samples obtained from Fundão dam's remains using various loading conditions (CID, CIU, and CAU) were performed by Morgenstern et al. [1]. The range of mean effective consolidation stress varied between 200 kPa and 600 kPa. The critical state friction angle (ϕ'_{cs}) was equal to 33°. Four static DSS tests and three direct shear tests were performed in similar samples. The critical friction angle in DSS tests ranged from 28° to 32° for vertical consolidation stresses between 150 kPa and 600 kPa. In the direct shear tests, the mobilized friction angle at the end of the tests was 32° for vertical consolidation stresses between 250 kPa and 1350 kPa. Rezende [24] conducted drained triaxial compression and extension tests on undisturbed samples from the Fundão dam, obtained in three different locations at the beach before the collapse of the dam. Twelve tests reached the critical state and ϕ'_{cs} ranged from 32° to 36° for mean consolidation stresses varying from 75 kPa to 550 kPa. Wagner et al. [25] tested sand tailings from Minas Gerais state in triaxial extension and triaxial compression tests. ϕ'_{cs} varied from 33.4° to 35.8°.

2.2. Correlations between Piezocone Results and Sand Parameters

In this work, CPTu results were used to estimate ϕ' and D_r of the sand tailings from the Germano dam, as explained below.

Given the massive size and significant heterogeneity of tailings reservoirs, CPTu tests are widely used for profiling and properties estimation by correlations. The chart shown in Figure 3 is usually employed to estimate the grain size of the tailings. In this work, materials with $I_c < 2.6$ of the types 5 and 6 (i.e., sand-mixtures, sand) were classified as sand tailings [26], according to Equation (1):

$$I_c = \sqrt{\{3.47 - log(Q_t)\}^2 + \{1.22 + log(F_r)\}^2} \quad (1)$$

Q_t is the normalized tip resistance, and F_r is the normalized friction ratio [26–28].

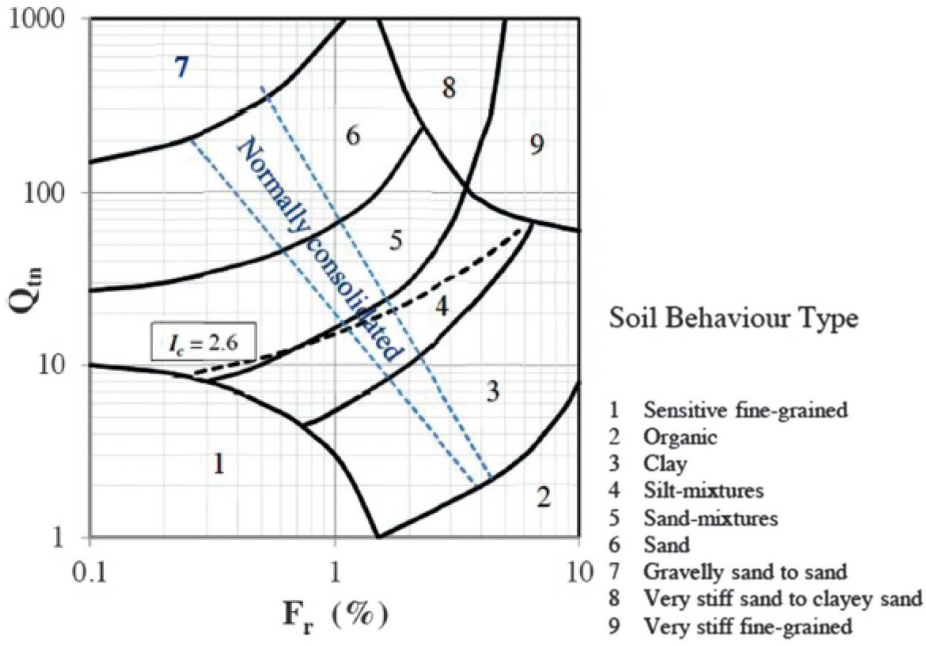

Figure 3. Soil classification chart [29,30].

The relative density, D_r, is a common measure of the degree of packing of sands and is loosely related to the peak friction angle. In young, uncemented, silica-based sands D_r may be estimated from the normalized cone resistance (Q_{tn}) by Equation (2) [31].

$$D_r = \sqrt{\frac{Q_{tn}}{350}} \quad (2)$$

There are several correlations to estimate the effective friction angle. Two equations were used in this research because they are well-known and widely accepted. Equation (3) was developed by Kulhavy and Mayne for uncemented, clean, rounded sands [32] based on the assessment of flexible walled CPT calibration chamber test data.

$$\phi' = 17.6 + 11log(Q_{tn}) \quad (3)$$

Previously, Equation (4) was developed by Robertson and Campanela [33] to estimate the peak friction angle based on spherical cavity expansion theory and a limit plasticity formulation.

$$\phi' = \arctan\left[0.1 + 0.38 \cdot log\left(\frac{q_t}{\sigma'_{vo}}\right)\right] \quad (4)$$

The corrected cone resistance is represented by q_t.

2.3. Effect of Layers of Plastic Tailings Amidst the Sand Tailings

Experimental studies [34,35] have shown that the cone tip resistance is influenced by the material properties ahead and behind the penetrating cone. Therefore, CPTu measurements in the sand tailings are affected as the cone approaches or exits a plastic, clay-like layer.

Experimental observations have shown that, in soft materials, the diameter of the zone of influence can be as small as two or three cone diameters, while it can reach 10–20 cone diameters in stiff materials [36].

Numerical analyses for two-layer soils composed of sand and clay have shown that the interface influence distance varies, in sands, according to the relative densities and horizontal stress state [37]. From that study, it was possible to infer the interface influence distance as a function of the relative density of the sand, as depicted in Figure 4.

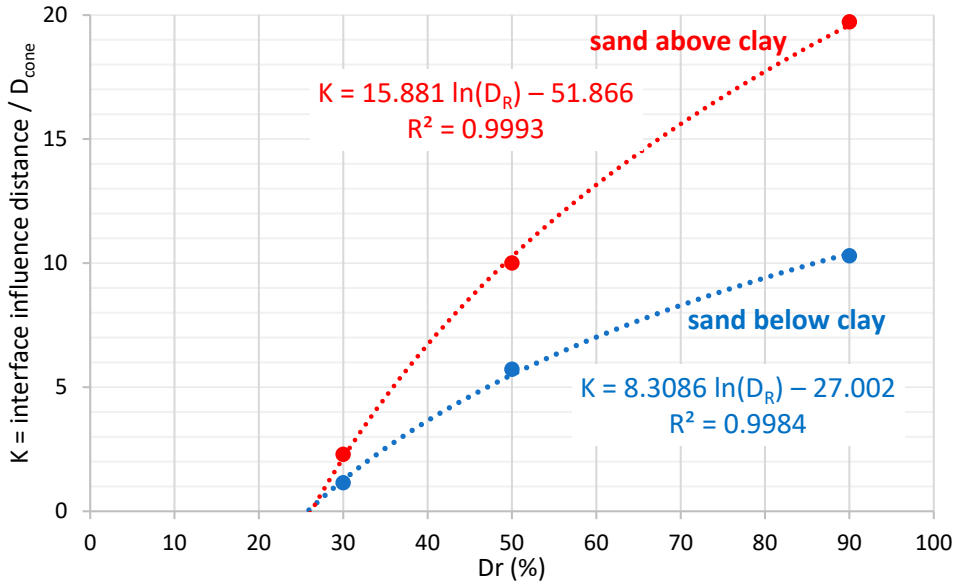

Figure 4. Interface influence distances in the sand, based on [37].

The influence of a plastic layer below the sand layer is usually more significant than that of a plastic layer above it. However, Figure 4 suggests that the presence of plastic layers above or below shall not influence the cone resistance of the sand layer if the relative density is equal to or less than 26%.

2.4. Data Treatment

The present work was developed with data from CPTu tests conducted in the main reservoir of the Germano dam presented in Appendix C1 of the report on the immediate causes of the Fundão dam failure [1]. Details pertaining to the CPTu equipment and test location can be found in the original reference. Values of q_t and f_s were obtained from the test bulletins at each centimeter with the aid of the WebPlotDigitizer v4.5 software.

The tailings disposal process and point of discharge frequently change over time, resulting in layers of plastic, clay-like tailings irregularly distributed amidst the sand tailings in the reservoir. The present work studies only the sand tailings of the Germano reservoir. Therefore, excluding the CPTu data from the plastic layers was necessary by discarding data with $I_c \geq 2.6$ [15].

For each centimeter of data from the available CPTu tests that presented $I_c < 2.6$, the peak effective friction angle was estimated using Equations (3) and (4).

Due to a disposal procedure used from 2003 to 2005, there is a continuous layer of plastic tailings about El. 900 m with 3 m to 4 m of thickness. The upper and lower layers consist primarily of sand tailings and were named Layers 1 and 2, respectively. Layer 2 presents many thin layers of plastic tailings, while Layer 1 does not show as many plastic intercalations. In all tests, the estimated friction angle close to the surface was exaggeratedly high, especially by Equation (4). The low effective stress probably causes this, and these data were discarded. A typical CPTu friction effective angle profile of sand tailings is shown in Figure 5, in which "n" indicates the number of measurements.

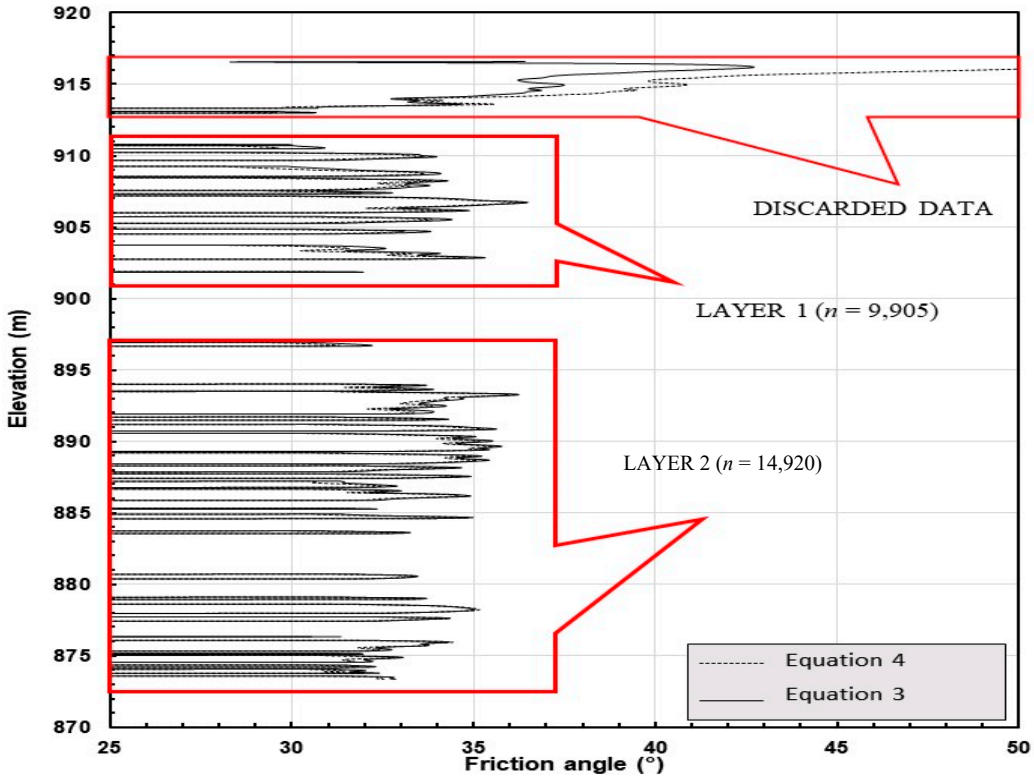

Figure 5. Estimated effective friction angle of sand tailings–CPTu-F16 according to Equations (3) and (4).

3. Results

Four different scenarios of analysis were studied to assess which would better characterize the coarse tailings of the Germano Dam:

- Scenario 0: analysis of all measurements of materials classified as sand tailings; no exclusions.
- Scenario 1: discard outliers—values three standard deviations above or below the mean i.e., $\mu \pm 3\sigma$, were removed (approximately 0.3% of the data were discarded).
- Scenario 2: discard measurements possibly influenced by the layers of plastic, clay-like tailings above and below the sand—readings within the first 0.2 m and the last 0.35 m of any sand tailings layer were discarded, according to the criteria proposed by [37]. A relative density of 50% was adopted conservatively.
- Scenario 3: combined analysis of scenarios 1 and 2, i.e., values three standard deviations above or below the mean were removed after discarding measurements possibly influenced by the layers of plastic tailings.

3.1. Scenario 0

The relative density of the sand tailings based on Equation (2) for young uncemented sands is presented in Figure 6. A log-normal distribution can be seen despite some dispersion. The relative density ranges from very loose to medium. Dense sand tailings were very rare. The total number of data points is n = 24,825.

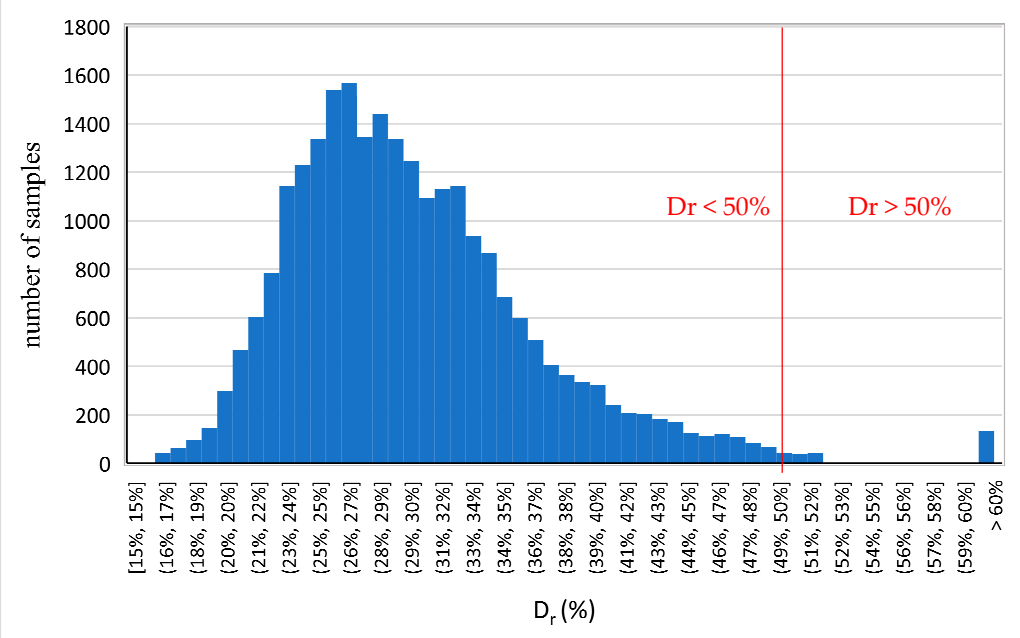

Figure 6. Histogram of the relative density of the sand tailings data.

The adjusted normal frequency distributions for the effective friction angle estimated by correlations [32,33] are presented in Figure 7 (cold and hot colors, respectively), combined for both layers and individually. The dashed lines represent the data frequency distribution.

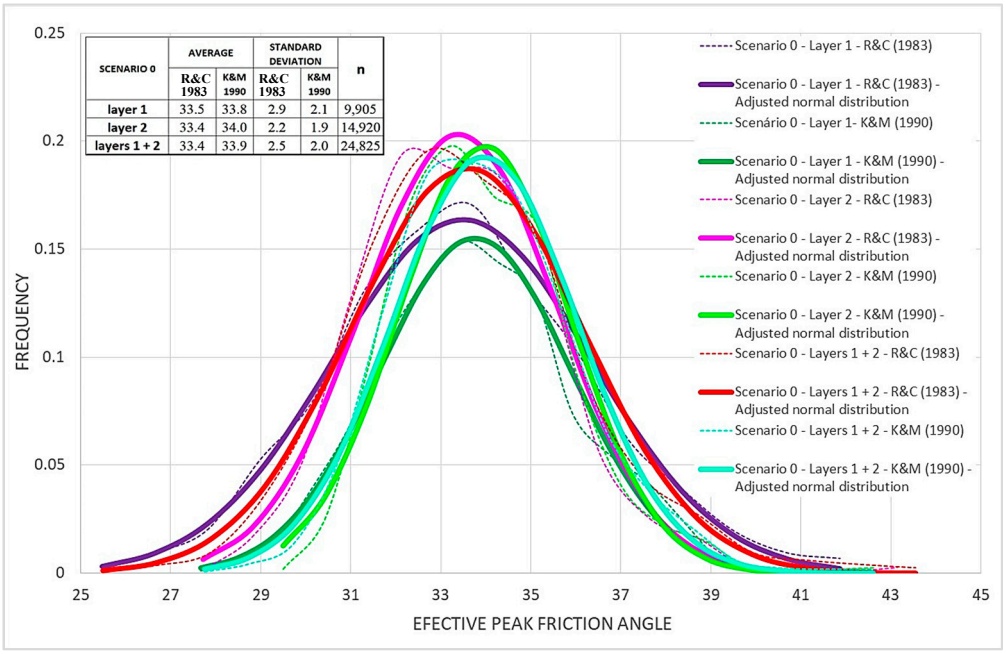

Figure 7. Scenario 0–Frequency distribution of the peak friction angle of the sand tailings [32,33].

3.2. Scenario 1

In this scenario, the outliers ($\phi' > \mu + 3\sigma$ and $\phi' < \mu - 3\sigma$) were not considered. A total of 24,681 data points remained in the sample (98.9% of the total).

The normal frequency distribution for the effective friction angle estimated by correlations proposed by correlations [32,33] in hot colors are presented in Figure 8, combined and individually for each layer, along with the data frequency distribution depicted in the dashed lines. The discard of the outliers resulted in less variability in the frequency distribution curves. Nevertheless, the differences between the adopted correlations remain. It should be noted that the inferior layer (2) had a greater number of outliers, confirming its heterogeneity.

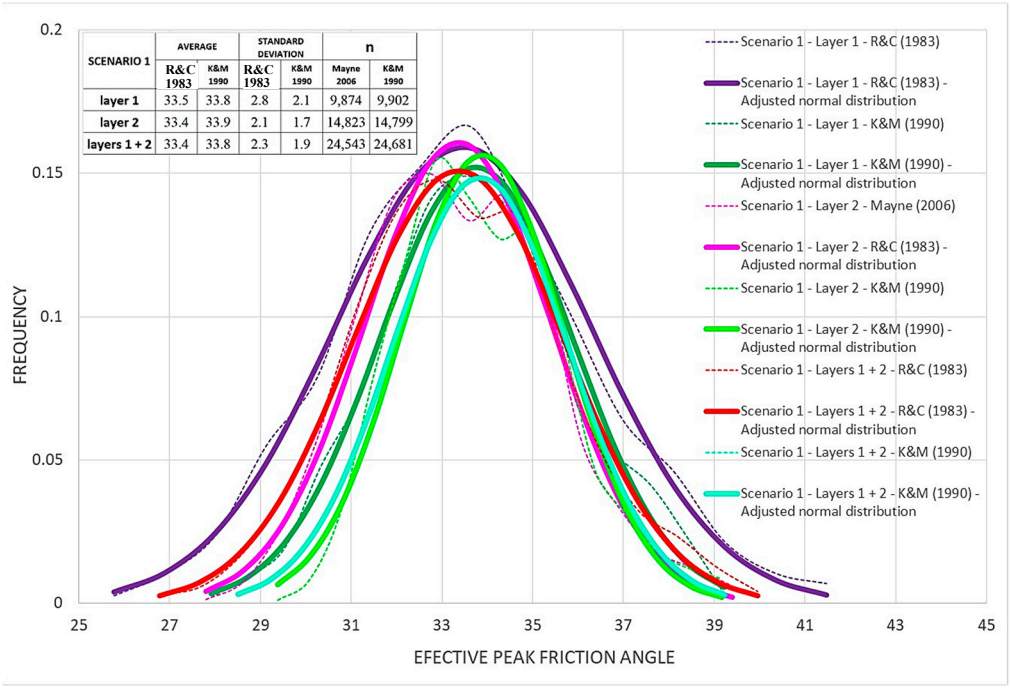

Figure 8. Scenario 1–Normal frequency distribution of the peak friction angle for the sand tailings [32,33].

3.3. Scenario 2

In this scenario, the first 0.2 m of sand tailings data after a plastic layer were eliminated, as well as the last 0.35 m before the next plastic tailings layer. This was done to eliminate the effects of the plastic tailings on the CPTu readings in the sand tailings that are close to the boundaries of their sand layer. Sand tailings layers with less than 0.55 m of thickness were disregarded entirely. A relative density of 50% was adopted to define the discard distance [37]. This resulted in the exclusion of 47.5% of the data in the sand layers above elevation 900 m and 67.5% in the layers below. A total of 10,052 data points remained in the sample.

The normal frequency distribution for the effective friction angle estimated by correlations proposed by [32] in cold colors and [33] in hot colors are presented in Figure 9, combined and individually for each layer, along with the data frequency distribution depicted in the dashed lines.

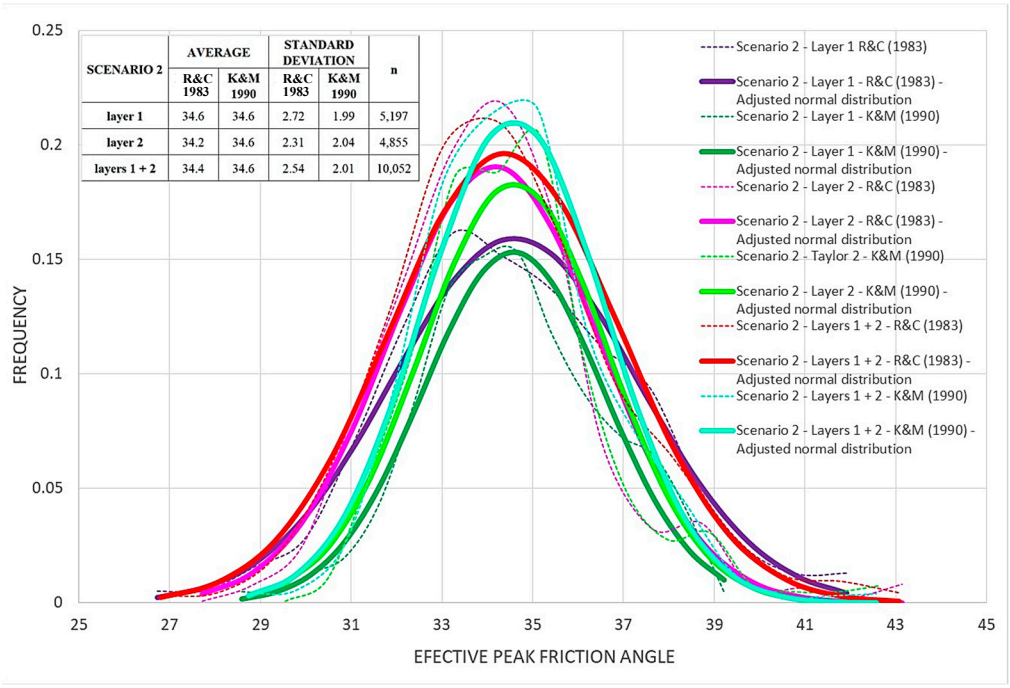

Figure 9. Scenario 2–Normal frequency distribution of the peak friction angle for the sand tailings [32,33].

3.4. Scenario 3

This scenario is a combination of scenarios 1 and 2, using the same criteria. First, the boundary values were excluded, and then the outliers were discarded.

This scenario excluded a quantity of data slightly larger than the previous one (47.7% of the data in the sand layers above elevation 900 m and 68.0% in the layers below it). A total of 9946 data points remained in the sample.

The normal frequency distribution for the effective friction angle estimated by correlations proposed by [32] in cold colors and [33] in hot colors are presented in Figure 10, combined and individually for each layer, along with the data frequency distribution depicted in the dashed lines.

The discard of more than 50% of the data resulted in the irregular distribution of the data frequency but reduced the discrepancy between the mean values and standard deviations when comparing the different correlations as well as among the individual and combined approach for the layers.

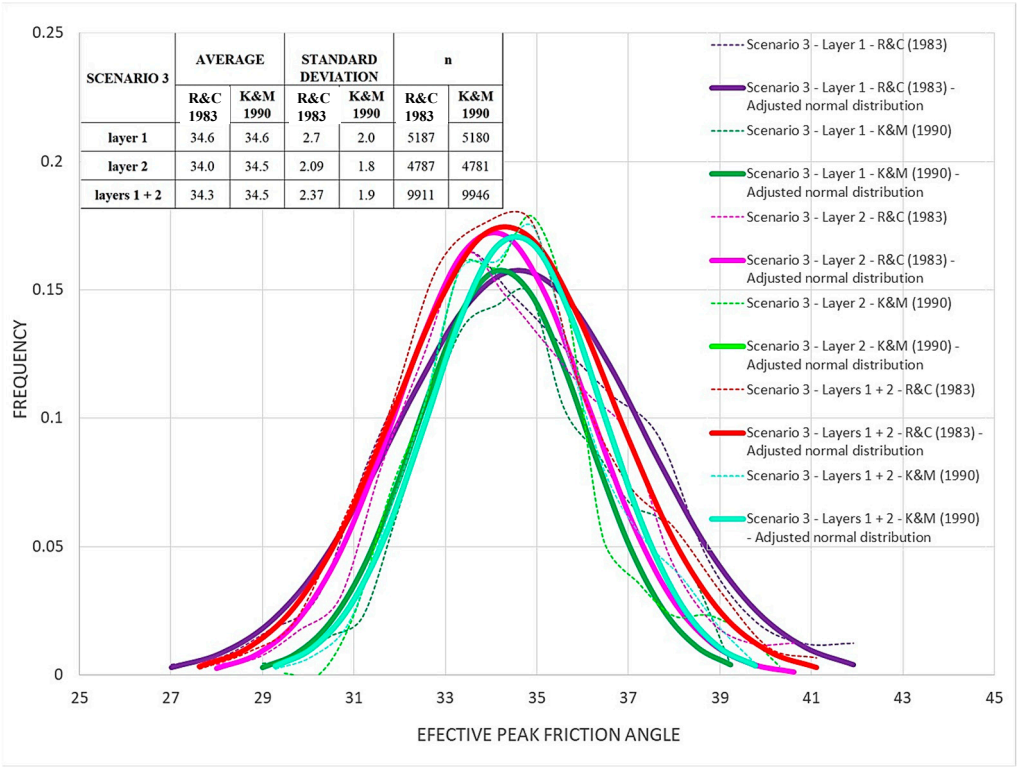

Figure 10. Scenario 3–Normal frequency distribution of the peak friction angle for the sand tailings [32,33].

4. Discussion

Despite the low Dr, relatively high values of ϕ′ were obtained in all evaluated scenarios. The angularity of the particles may explain this. Sharp particles of quartz and iron oxide can be seen in the sand tailings from the Fundão dam (Mariana, Brazil) in images obtained by electronic microscope (Figure 2) [20]. The optical microscope [19] revealed a similar pattern of particles of high angularity (Figure 1). X-ray diffraction indicated that the sand tailings of the Germano dam are composed almost entirely of hematite and quartz [38]. This result is in good agreement with X-ray fluorescence performed on the sand tailings from Fundão dam [20]. It should be noted that both dams received tailings from the same mine.

Although Equation (3) was proposed for sands with round grains [32], the results obtained herein are compatible with triaxial and direct shear tests [19–22]. Four different analysis scenarios were evaluated to assess the influence of the plastic tailings layers interspersed between the sand tailings, and the outliers. The friction angle distributions of all tests were similar to the normal distribution, with mild to moderate asymmetries. When all data was considered (scenario 0), the mean effective friction angle was 33.5° [33] and 34.0° [32]. It is worth mentioning that, in this scenario, there was a significant presence of high values. Samples retrieved from SPT tests revealed some pebbles and rock fragments in the sand tailings [1] that might explain the high friction angles.

To eliminate the outliers, values above or below three standard deviations from the mean were discarded in scenario 1, resulting in a reduction in the mean of less than 0.1°. It is noteworthy that the asymmetry in this scenario remained slightly positive, showing a slight decrease in relation to the previous scenario.

For scenario 2, the measurements closer to the boundaries of the sand layers were excluded to eliminate the influence of the neighboring plastic tailings layers. In this scenario, a significant increase in the mean of approximately 1.0° [33], and 0.8° [32], indicating that the presence of plastic layers really influenced the tip resistance in neighboring sand tailings. Again, mild to moderate positive asymmetries were observed. It is also worth noting that the discard carried out in this scenario was possibly conservative since the average relative

compactness recorded in all scenarios was around 30%, but the adopted zones of influence corresponded to D_r = 50%.

Scenario 3 combined scenarios 1 and 2, resulting in a slight reduction of the mean.

Scenarios 2 and 3 showed more significant asymmetries for the sand tailings above an elevation of 900 m compared to scenarios 0 and 1. In comparison, for the sand tailings below elevation 900 m, there was a reduction in asymmetry in scenarios 2 and 3. This resulted in similarly combined asymmetries in the four scenarios.

In general, it was not possible to define patterns regarding the spatial distribution of the tailings that were likely caused by operational issues of tailings releases with considerable variation in discharge points and procedures to which this reservoir was subjected throughout its lifespan. Nevertheless, when all tests were analyzed together, the effective friction angle distribution fitted very well with a normal distribution. The distribution of the effective friction angle of the sand tailings of the Germano dam may be considered normal for the purposes of probabilistic analysis of slope stability since the asymmetry was always mild or moderate.

Furthermore, the distribution of the relative density of these tailings closely resembled a log normal. Since D_r is directly proportional to the square root of Q_{tn} (Equations (2) and (3)), the logarithm of the normalized tip resistance will have a normal distribution. Therefore, the friction angle, which is proportional to the logarithm of Q_{tn}, must present a normal distribution (multiplied by a constant), which was confirmed in this work.

The mean values for the effective friction angle obtained in this research varied between 33° and 35° in different analysis scenarios. These values were consistent and within the range of effective friction angles obtained in other iron ore tailings dams in the Brazilian Iron Quadrangle [1,18–25]. The discard of boundary measurements seems to be necessary since it increased the mean by approximately 1°. On the other hand, discarding outliers had little to no effect.

It is worth mentioning that, as observed in this work, most of the tailings have relative density below 40%, indicating that the calculated effective friction angle possibly corresponds to the critical state. Furthermore, the occurrence of relatively high values of friction angles, even in a loose state, agrees with the fact that these tailings have very angular grains, as indicated by the optical and electron microscope photographs [19,20].

5. Conclusions and Recommendations

The probability density functions of the effective friction angle and the relative density of sand tailings from the Germano dam main reservoir were estimated by correlations with the results of piezocone tests. Only CPTu data with $I_c < 2.6$ were considered. Outliers and readings close to the plastic clay-like layers were disregarded. The peak effective friction angle was estimated using Equations (3) and (4). The effective friction angle distribution fitted well with a normal distribution, and the distribution of the relative density closely resembled a log-normal.

The mean values for the effective friction angle obtained in this research varied between 33° and 35°, in good agreement with the range of effective friction angles of iron ore tailings dams in the same region of Brazil [1,18–25]. The standard deviation ranged between 1.9–2.5°.

The influence of the plastic tailings layers interspersed between the sand tailings was minimized by discarding the readings close to the boundaries of the sand layers, resulting in an increase of approximately 1° in the mean, without alteration to the standard deviation, thus indicating that this is a necessary step in the assessment of friction angle by CPTu.

When using CPTu correlations to evaluate ϕ' of sand tailings intermixed with clay-like layers, it is advisable to account for the influence of the clay-like layers.

Author Contributions: Conceptualization, L.D.B.B. and M.d.C.R.C.; methodology, L.D.B.B. and M.d.C.R.C.; formal analysis, L.D.B.B., M.d.C.R.C. and A.A.M.M.; data curation, A.A.M.M.; writing—original draft preparation, L.D.B.B., M.d.C.R.C. and A.A.M.M.; writing—review and editing, L.D.B.B. All authors have read and agreed to the published version of the manuscript.

Funding: This research received no external funding.

Data Availability Statement: Data sharing is not applicable to this article.

Conflicts of Interest: The authors declare no conflict of interest.

References

1. Morgenstern, N.R.; Vick, S.G.; Viotti, S.G.; Watts, B.D. Report on the Immediate Causes of the Failure of the Fundão Dam. 2016. Available online: https://www.resolutionmineeis.us/sites/default/files/references/fundao-2016.pdf (accessed on 20 December 2022).
2. El-Ramly, H.; Morgernstern, N.R.; Cruden, D.M. Probabilistic slope stability analysis for practice. *Can. Geotech. J.* **2002**, *39*, 665–683. [CrossRef]
3. Griffiths, D.V.; Fenton, G.A. Probabilistic slope stability analysis by finite elements. *J. Geotech. Geoenviron.* **2004**, *130*, 507–518. [CrossRef]
4. Cho, S.E. Probabilistic assessment of slope stability that considers the spatial variability of soil properties. *J. Geotech. Geoenviron.* **2009**, *136*, 975–984. [CrossRef]
5. Javankhoshdel, S.; Bathurst, R.J. Simplified probabilistic slope stability design charts for cohesive and cohesive-frictional (c-ϕ) soils. *Can. Geotech. J.* **2014**, *51*, 1033–1045. [CrossRef]
6. Chen, F.; Zhang, R.; Wang, Y.; Liu, H.; Böhlke, T.; Zhang, W. Probabilistic stability analyses of slope reinforced with piles in spatially variable soils. *Int. J. Approx. Reason.* **2020**, *122*, 66–79. [CrossRef]
7. Reale, C.; Xue, J.; Pan, Z.; Gavin, K. Deterministic and probabilistic multi-modal analysis of slope stability. *Comput. Geotech.* **2015**, *66*, 172–179. [CrossRef]
8. Hekmatzadeh, A.A.; Zarei, F.; Johari, A.; Haghighi, A.T. Reliability analysis of stability against piping and sliding in diversion dams, considering four cutoff wall configurations. *Comput. Geotech.* **2018**, *98*, 217–231. [CrossRef]
9. DeWolfe, G.F.; Griffiths, D.V.; Huang, J. Probabilistic and deterministic slope stability analysis by random finite elements. In *GeoTrends: The Progress of Geological and Geotechnical Engineering in Colorado at the Cusp of a New Decade*; American Society of Civil Engineers: Denver, CO, USA, 2010. [CrossRef]
10. Das, T.; Hegde, A. A Comparative Deterministic and Probabilistic Stability Analysis of Rock-Fill Tailing Dam. In *Advances in Computer Methods and Geomechanics. Lecture Notes in Civil Engineering*; Prashant, A., Sachan, A., Desai, C., Eds.; Springer: Singapore, 2020; Volume 55. [CrossRef]
11. CDA—Canadian Dam Association. *Dam Safety Guidelines*; CDA: Markham, ON, Canada, 2013; 82p.
12. ANCOLD—Australian National Committee on Large Dams. *Guidelines on Risk Assessment*; ANCOLD: Hobart, Tasmania, 2022; 122p.
13. Varnes, D.J. *Landslides Hazard Zonation: A Review of Principles and Practice*; UNESCO: Paris, France, 1984.
14. Robertson, P.K.; de Melo, L.; Williams, D.J.; Wilson, G.W. 2019. Available online: http://www.b1technicalinvestigation.com/report.html (accessed on 21 April 2020).
15. Aires, U.R.V.; Santos, B.S.M.; Coelho, C.D.; da Silva, D.D.; Calijuri, M.L. Changes in land use and land cover as a result of the failure of a mining tailings dam in Mariana, MG, Brazil. *Land Use Policy* **2018**, *70*, 63–70. [CrossRef]
16. do Carmo, F.F.; Kamino, L.H.Y.; Junior, R.T.; de Campos, I.C.; do Carmo, F.F.D.; Silvino, G.; de Castro, K.J.d.S.X.; Mauro, M.L.; Rodrigues, N.U.A.; Miranda, M.P.d.S.; et al. Fundão tailings dam failures: The environment tragedy of the largest technological disaster of Brazilian mining in global context. *Perspect. Ecol. Conserv.* **2017**, *15*, 145–151. [CrossRef]
17. Coimbra, K.T.O.; Alcântara, E.F.C.; Souza Filho, C.R. An assessment of natural and manmade hazard effects on the underwater light field of the Rio Doce River continental shelf. *Sci. Total Environ.* **2019**, *685*, 1087–1096. [CrossRef] [PubMed]
18. Albuquerque Filho, L.H. Avaliação do Comportamento Geotécnico de Barragens de Rejeitos de Minério de Ferro Através de Ensaios de Piezocone. Master's Thesis, Universidade Federal de Ouro Preto, Ouro Preto, Brazil, 2004.
19. Becker, L.B.; Fabre, J.S.; Barbosa, M.C. Determination of the critical state of a silty sand iron tailings in triaxial extension tests using photographic correction. *Can. Geotech. J.* **2022**. [CrossRef]
20. Flórez, C. Estudo da Alteração em Laboratório de Rejeitos de Mineração de Ferro para Análise em Longo Prazo. Ph.D. Thesis, Federal University of Rio de Janeiro, Rio de Janeiro, Brazil, 1 December 2015.
21. Becker, L.D.B.; Barbosa, M.C. Undrained Behavior of Fundão Sandy Iron Tailings. *Soils Rocks* 2023, *submitted*.
22. Quintelas, A.C.F.; Becker, L.B.; Moura, M.V.S. The influence of relative density on the friction angle of iron ore tailings from the Fundão Dam. In Proceedings of the XIII International Symposium on Landslides, Cartagena, Colombia, 22–26 February 2021.
23. Quirino, I.S.; Fabre, J.S.; Becker, L.D.B.; Barbosa, M.C. Análise da Influência do Teor De finos no Ângulo de Atrito de um Rejeito de Minério de Ferro Através de Ensaios Ring Shear. In Proceedings of the XX Congresso Brasileiro de Mecânica dos Solos e Engenharia Geotécnica, Campinas, Brazil, 23–26 August 2022.

24. Rezende, V.A. Estudo do Comportamento de Barragem de Rejeito Arenoso Alteada por Montante. Master's Thesis, Universidade Federal de Ouro Preto, Ouro Preto, Brazil, 2013.
25. Wagner, A.C.; Silva, J.P.D.S.; Carvalho, J.V.D.A.; Rissoli, A.L.C.; Cacciari, P.P.; Chaves, H.M.; Filho, H.C.S.; Consoli, N.C. Mechanical behavior of iron ore tailings under standard compression and extension triaxial stress paths. *J. Rock Mech. Geotech. Eng.* **2022**, *in press*. [CrossRef]
26. Robertson, P.K.; Wride, C.E. Evaluating cyclic liquefaction potential using the cone penetration test. *Can. Geotech. J.* **1998**, *35*, 442–459. [CrossRef]
27. Wroth, C.P. Interpretation of In Situ soil test, 24th Rankine Lecture. *Geotéchnique* **1984**, *34*, 449–489. [CrossRef]
28. Houlsby, G. *Discussion Session Contribution Penetration Testing in the U.K. Birmingham*; Thomas Telford: London, UK, 1988; pp. 141–146.
29. Robertson, P.K. Interpretation of cone penetration tests—Unified approach. *Can. Geotech. J.* **2009**, *46*, 1337–1355. [CrossRef]
30. Robertson, P.K. Cone Penetration Test (CPT)-Based Soil Behavior Type (SBT) Classification System—An Update. *Can. Geotech. J.* **2016**, *53*, 1910–1927. [CrossRef]
31. Robertson, P.K.; Cabal, K.L. *Guide to Cone Penetration Testing for Geo-Environmental Engineering*; Gregg Drilling & Testing Inc.: Martinez, MA, USA, 2010.
32. Kulhawy, F.H.; Mayne, P.W. *Manual on Estimating Soil Properties for Foundation Design*; Cornell University: Ithaca, NY, USA, 1990.
33. Robertson, P.K.; Campanella, R.G. Interpretation of Cone Penetration Tests: Sands and Clays. *Can. Geotech. J.* **1983**, *20*, 719–745. [CrossRef]
34. Treadwell, D.D. The Influence of Gravity, Prestress, Compressibility, and Layering on Soil Resistance to Static Penetration. Ph.D. Thesis, University of California, Berkeley, CA, USA, 1976.
35. Van der Linden, T.I.; De Lange, D.A.; Korff, M. Cone penetration testing in thinly inter-layered soils. *Proc. Inst. Civ. Eng.–Geotech. Eng.* **2018**, *171*, 215–231. [CrossRef]
36. Lunne, T.; Robertson, P.K.; Powel, J.J.M. *Cone Penetration Testing in Geotechnical Pratice*, 2nd ed.; Taylor and Francis Group: London, UK, 1997.
37. Ahmadi, M.M.; Robertson, P.K. Thin-layer effects on the CPT qc measurement. *Can. Geotech. J.* **2005**, *42*, 1302–1317. [CrossRef]
38. Motta, H.P.G. Comportamento de um Rejeito de Transição em Centrífuga Geotécnica. Master's Thesis, Universidade Federal do Rio de Janeiro, Rio de Janeiro, Brazil, 2008.